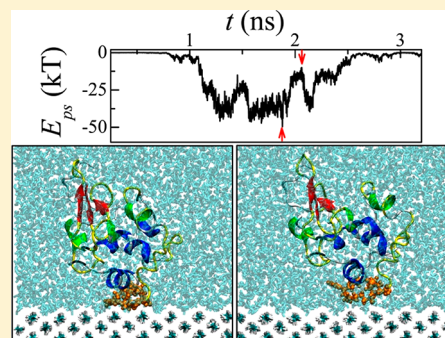


# Molecular Dynamics Simulation of Lysozyme Adsorption/Desorption on Hydrophobic Surfaces

Tao Wei, Marcelo A. Carignano, and Igal Szleifer\*

Department of Biomedical Engineering, Department of Chemistry and Chemistry of Life Processes Institute, Northwestern University, Evanston, Illinois 60208, United States

**ABSTRACT:** In this work, we present a series of fully atomistic molecular dynamics (MD) simulations to study lysozyme's orientation-dependent adsorption on polyethylene (PE) surface in explicit water. The simulations show that depending on the orientation of the initial approach to the surface the protein may adsorb or bounce from the surface. The protein may completely leave the surface or reorient and approach the surface resulting in adsorption. The success of the trajectory to adsorb on the surface is the result of different competing interactions, including protein–surface interactions and the hydration of the protein and the hydrophobic PE surface. The difference in the hydration of various protein sites affects the protein's orientation-dependent behavior. Side-on orientation is most likely to result in adsorption as the protein–surface exhibits the strongest attraction. However, adsorption can also happen when lysozyme's longest axis is tilted on the surface if the protein–surface interaction is large enough to overcome the energy barrier that results from dehydrating both the protein and the surface. Our study demonstrates the significant role of dehydration process on hydrophobic surface during protein adsorption.



## INTRODUCTION

The problem of protein adsorption at the solid–liquid interfaces has been the subject of intense studies, mainly due to its role and important implications in the design of biocompatible materials,<sup>1</sup> biosensors,<sup>2</sup> and drug delivery systems.<sup>3</sup> Protein adsorption is also an interesting and important fundamental problem because it is the result of the interplay between various interactions, hydration, and the ability of the proteins to change conformation upon adsorption. Many experimental efforts have addressed different aspects of the adsorption process, including its kinetics characteristics,<sup>4,5</sup> the structural deformation of the protein,<sup>4</sup> and the effects of the surface's chemistry<sup>6</sup> and morphology<sup>7</sup> in the multilayer or aggregate state. Despite these efforts, the experimental observation of single-protein adsorption at the microscopic details of the process remains a very challenging task. Molecular dynamics (MD) simulations are capable of providing spatial details at the atomic level as well as a time resolution spanning from subnanosecond to microseconds or even milliseconds, the latter achieved only for small proteins in solution with special purpose computational resources.<sup>8</sup> However, the very large number of water molecules in the system makes systematic studies of the adsorption process very challenging. It is possible to speed up the simulations of protein adsorption by adopting a two-step approach<sup>9–12</sup> consisting of (i) an implicit solvent energetic study on protein–surface complex to determine the most favorable protein's orientations and positions on the adsorbing surface and (ii) full atomistic simulations on selected conformations to relax the protein's structure in explicit water. Nevertheless, these methods, designed to avoid very long simulations, ignore the first stages of the adsorption process.

Recently, we reported a simulation study<sup>13</sup> for the adsorption of lysozyme onto a hydrophobic crystalline polyethylene (PE) surface, where we concentrated only on trajectories that resulted in adsorption. It was observed that the water molecules trapped between lysozyme and the hydrophobic PE surface need to be removed before the protein comes into full contact with the surface. This process of dehydration, for the cases in which the protein landed in a favorable orientation for adsorption, last more than 70 ns, and it is accompanied by a transformation of the protein secondary structure.<sup>13</sup> Several other factors, including surface hydrophobicity,<sup>13–15</sup> charge distribution,<sup>14,15</sup> and morphology<sup>13</sup> and their effect on the translational and rotational motions of the adsorbed protein have been studied by various research groups using atomistic simulations.

In this work, we present simulation results to study how the orientation of the proteins approaching the surface determines a successful (or unsuccessful) adsorption process, with particular emphasis on the role that the hydration plays on protein adsorption. In particular, we concentrate our attention on what are the orientations in which proteins adsorb to the surface versus those in which they do not. In this latter case, the protein bounces back to the solution, where it may reorient before approaching the surface for a second time, possibly in an adsorbing orientation. To study this effect, a series of full atomistic MD simulations was carried out, starting with the protein in a large variety of orientations away from the surface.

**Received:** April 26, 2012

**Revised:** August 4, 2012

**Published:** August 12, 2012



In this way, we can study how the initial orientation affects the successful adsorption or the rejection from the surface. We present in this article the longest set, to the best of our knowledge, of simulations dedicated to protein adsorption. This extensive study has allowed us to identify a new scenario in which the protein bounces on the attractive surface, rotates, and approaches the surface again in a different orientation more favorable for adsorption. The analysis of this process sheds light on the effect of the protein and surface dehydration on the free energy for protein adsorption.

## METHODS

MD simulations were performed using the Gromacs (version 4.0.7) simulation package,<sup>16</sup> and the resulting trajectories were analyzed using our own scripts. The interactions in the system were described by the OPLS-AA force field,<sup>17</sup> combined with the TIP4P water model.<sup>18</sup> The integration of the dynamic equations was done using the leapfrog algorithm, with a time step of 1 fs. The simulations were done under NVT conditions, with the temperature maintained at 300 K through coupling to a Berendsen thermostat. A spherical cutoff at 1.2 nm was imposed on all intermolecular interactions. A PE surface (010) was constructed by periodic expansion of the ethylene unit cell ( $0.7388 \times 0.4929 \times 0.239$  nm).<sup>19</sup> The atoms of the ethylene monomers near the edges of the periodic box were covalently bonded with those of the monomer's periodic images, mimicking infinitely long chains. The equilibrated PE surface structure in water has a thickness of 2.575 nm. The protein coordinates were downloaded from the crystal structure 1AKI from the Protein Data Bank (<http://www.ncbi.nlm.nih.gov/>). The amino acids histidine (His), arginine (Arg), and lysine (Lys) were protonated, whereas glutamate (Glu) and aspartate (Asp) were deprotonated, resulting in a net charge of +8e that corresponds to the experimental conditions at pH 7. The N and C termini were capped uncharged.

The simulation system, shown in Figure 1, was prepared as in our previous work.<sup>13</sup> For the present study, we considered an ensemble of 27 different initial orientations for the lysozyme, all of which fully solvated and were far enough from the surface so that they have negligible surface–protein interactions ( $E_{ps} \approx 0$  kT). Any water molecule within 0.3 nm of the lysozyme was removed. The system was neutralized by adding 8  $\text{Cl}^-$  ions. The interaction between the simulation box and its periodic images along the Z direction was effectively removed by inserting a vacuum slab of 2.5 nm on the top of the water box. Water molecules were kept inside the box by inserting a restraining layer of repulsive Lennard-Jones artificial atoms at fixed positions. Such settings resulted in a water slab of 8.5 nm from the top of the PE layer up to the restraining layer, sufficient to guarantee enough space for the protein to rotate inside the cell without being affected by the top, restraining layer.

The simulations were started with the relaxation of water molecules by running an energy minimization, followed by a short run of MD (50 ps) at 300 K, maintaining PE and lysozyme fixed. Then, the PE surface and water were relaxed with a series of simulations of 800 ps, using the annealing protocol starting with a temperature of 10 K and reaching 300 K in 10 steps. In this way, the whole system (protein and the surface) was hydrated without any perturbation of the protein structure. Finally, production runs were carried out in the NVT ensemble at 300 K, using a 1 fs time step.

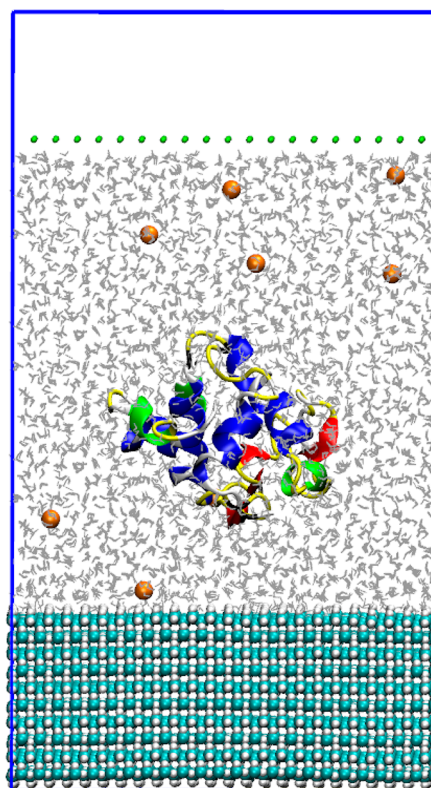


**Figure 1.** Snapshot of the simulation system at  $t = 0$  for one of the simulated trajectories. The box dimensions are  $6.565 \times 6.119 \times 11.3$  nm<sup>3</sup> ( $X \times Y \times Z$ ): lysozyme on PE surface (010) in water (gray) and counterions,  $\text{Cl}^-$  (orange), capped with repulsive wall (green), projected in the  $Y$ – $Z$  plane. The polyethylene chains are aligned in the direction of the  $Y$  axis. The  $Z$  direction is normal to the PE surface.

## RESULTS

Our previous study<sup>13</sup> showed a single trajectory of 300 ns, in which the lysozyme is being adsorbed onto the surface after a side landing, namely, with the longest axis being parallel to the surface. To increase our understanding of lysozyme's adsorption behavior on hydrophobic PE surface, in this work we performed 27 simulations with different initial orientations of the protein relative to the surface. Of these 27 different trajectories, 13 cases resulted in adsorption within a time of 200 ns. In the remaining 14 cases, the lysozyme diffused away from the surface. The adsorption angle,  $\theta$  ( $-90^\circ \leq \theta \leq 90^\circ$ ) is defined as the angle between the PE surface and the principal axis of inertia drawn from the protein center of mass toward the residue Arg128. This particular residue was chosen as reference because it is consistently close the main principal axis of inertia.<sup>13</sup> The protein–surface distance,  $z_{ps}$ , is defined as the closest distance between the protein and the center of the mass of the carbon atoms of the top PE layer. We analyzed all of the trajectories beginning with the protein above the surface, until the protein either fully reached the surface with a stable orientation (adsorption cases) or failed to adsorb after 100 ns (nonadsorption cases). In Figure 2, we show the collective information of the proteins' trajectories as a density map in the  $\theta$ ,  $z_{ps}$  plane. The quantity  $I_{oc}$  represents the frequency of visiting a particular pair ( $\theta$ ,  $z_{ps}$ ) for all of the 27 trajectories up to 40 ns. We restrict the analysis to the close vicinity to the surface, specifically  $z_{ps} < 0.6$  nm. The Figure shows that the protein spends most of the time in the region adjacent to the surface,

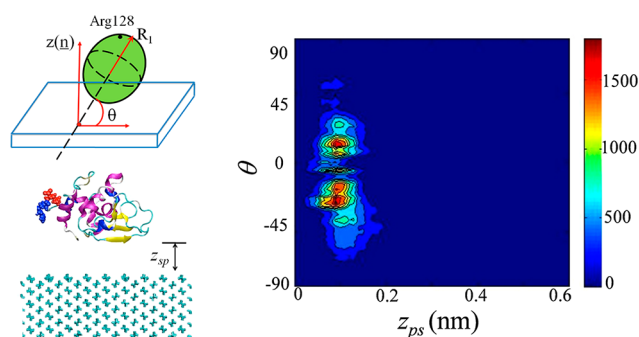


**Figure 2.** Left: Definition of the protein–surface relative orientation,  $\theta$ , and protein–surface distance,  $z_{ps}$ . Right: contour map of the frequency of the protein visiting,  $I_{oc}$ , as a function of  $\theta$  and  $z_{ps}$  calculated from all 27 cases during the first 40 ns of simulation. Contour map of the frequency of the protein visiting,  $I_{oc}$ , as a function of the orientation,  $\theta$ , and distance from the surface,  $z_{ps}$ , calculated from all 27 cases during the first 40 ns of simulation. The grid spacing is  $2^\circ$  and 0.01 nm for  $\theta$  and  $z_{ps}$ , respectively.

namely, for  $0.1 \text{ nm} < z_{ps} < 0.15 \text{ nm}$ . The reason for this behavior, as it was shown in ref 13 and will be expanded below, is the long time needed to remove the water molecules trapped between the protein and the surface, which is often accompanied by a rotation and deformation of the protein. Figure 2 shows that lysozyme is mostly likely to be adsorbed when it lands on its side ( $\theta \approx 0^\circ$ ). It is also interesting to note that the orientation distribution of the adsorbed lysozyme on the PE surface is rather asymmetric: no adsorption is observed at the regions of  $45^\circ < \theta < 90^\circ$  and  $-90^\circ < \theta < -70^\circ$  on PE surface. The collective analysis of our simulations, which represent a small sampling in statistical terms, points to a clear asymmetry in the orientation of the protein at landing and the success of the adsorption process.

The protein–surface interaction energy ( $E_{ps}$ ), calculated from the same set of trajectories used for Figure 2, is displayed in Figure 3 as a function of  $\theta$  and  $z_{ps}$ . For this plot, we extend

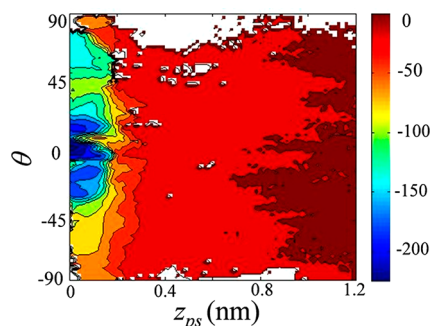


**Figure 3.** Contour map of the protein–surface interaction energy,  $E_{ps}$ , as a function of  $\theta$  and  $z_{ps}$  calculated from all 27 trajectories during the first 40 ns of simulation. The color scale is in units of kT. White color represents lack of data.

the range of  $z_{ps}$  values to reach the region of negligible protein–surface attraction. Figure 3 shows that for interaction energies larger than  $-50 \text{ kT}$  (red zone) the protein has no preferential orientation. In other words, for distance from the surface larger than 0.3 nm, the protein–surface interactions are independent of the angle. The lack of data for  $\theta \approx 90^\circ$  is due to the limited statistics and not related to a preferential orientation far from the surface. The protein feels a significant energetic

attraction for  $z_{ps} < 0.3 \text{ nm}$  with the most favorable orientation at  $\theta \approx 0^\circ$ , where the energies are much lower and the probability is much higher; see Figure 2. The distribution of  $E_{ps}$  on PE surface is inhomogeneous, similarly to our previous observation<sup>13</sup> for a single adsorbing trajectory. Note that Figures 2 and 3 represent data including the protein in solution in the early stage of the process. Namely, the Figures do not include data corresponding to the long deformation process that takes place after the lysozyme adsorbs irreversibly onto the PE surface, which takes more than 100 ns. The protein–surface interaction energy decays to a negligible value for separations  $z_{ps} > 0.6 \text{ nm}$ . As expected, there is correspondence between  $I_{oc}$  and  $E_{ps}$ . The most frequently visited region in the  $\theta$  and  $z_{ps}$  plane corresponds to conformations of low protein–surface interaction energy. Certainly, the protein surface interaction is an important factor determining the adsorption behavior, but there are other contributions that may play a role.

The fully solvated protein is surrounded by a layer of condensed water. We analyze the protein's hydration using the proximal radial distribution function,  $pG(r)$ .<sup>13</sup> This is a pair correlation function between the protein atoms and the solvent molecules closest to the protein's atom. Then,  $pG(r)$  is a measure of the solvent structure in the proximity of the protein–solvent interface. According to the proximal radial distribution function of oxygen atoms,  $pG(r)$ , the hydration layer has its peak at 0.3 nm from the protein's surface.<sup>13,20–22</sup> Water molecules within this hydration shell are hydrogen bonded to the protein, mainly as donors but some of them as acceptors.<sup>13</sup> In all 13 trajectories that lead to adsorption, the water molecules trapped between the protein and hydrophobic PE surface are slowly removed upon lysozyme adsorption. We find that from all of the successful adsorbing cases those characterized by side landing show the dehydration to be the rate-determining step for the complete adsorption to the surface, similarly to what we observed before.<sup>13</sup> In some cases in which the protein approaches the surface in an orientation unfavorable for adsorption, we have observed the protein to bounce out of the surface, change its orientation, and approach the surface a second time. One of these cases is exemplified in Figure 4, where we show the motion of the lysozyme as represented by the distance to the surface ( $z_{ps}$ ) and the adsorption angle ( $\theta$ ), along with the protein–surface interaction energy ( $E_{ps}$ ). The Figure shows that the protein approaches the surface and attempts three landings, and only the last one is successful in terms of adsorption. In the first two landings, the lysozyme is eventually repelled away from the surface. The adsorption angle  $\theta$  is approximately  $-43^\circ$  and  $-8^\circ$  for the first two landings, respectively. Even though the PE surface exerts a significant attraction to the lysozyme during the first two landings, namely,  $E_{ps} \approx -50 \text{ kT}$  and  $E_{ps} \approx -22 \text{ kT}$  for first and second attempts, respectively, the protein is still unable to reach the surface within a distance ( $z_{ps}$ ) smaller than 0.25 nm. In the two cases, the protein bounces away and reorients above the surface. The third landing attempt is with the longest axis tilted on the surface ( $\theta \approx 38^\circ$ ), and it shows a steady decrease in the protein–surface interaction energy reaching  $E_{ps} \approx -65 \text{ kT}$  in  $\sim 1 \text{ ns}$ . Then, the system proceeds with the dehydration stage that last for 12 ns, after which the adsorption angle stabilizes at  $13.2^\circ$ . Compared with our previous case of side landing,<sup>13</sup> which takes  $\sim 70 \text{ ns}$  in the dehydration phase, the tilted landing yields to a faster complete adsorption. The reason could be related to the difference in hydration of the respective landing sites. For the tilted landing case, the protein



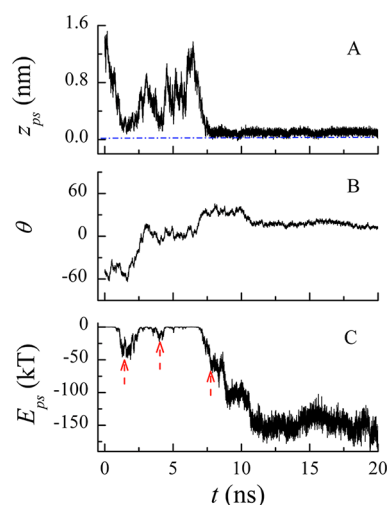


**Figure 4.** Example of a process of lysozyme adsorption that involves two unsuccessful attempts before a third landing that results in adsorption. The entire process is monitored by looking at the protein–surface distance  $z_{ps}$  (A), the adsorption angle  $\theta$  (B), and the protein–surface interaction energy  $E_{ps}$  (C).

has fewer residues adjacent to the PE surface than in the side landing case; therefore, a smaller number of water molecules have to be removed. After the third landing, the protein–surface interaction energy ( $E_{ps}$ ) decreases in an approximately stepwise pattern reflecting the structural rearrangements of the adsorbed lysozyme. It is important to emphasize that the decrease in energy after the successful adsorption event is very sharp, reaching very large attractive interactions with the surface within a few nanoseconds.

In Figure 5, we show the distance between the center of mass of every residue and the adsorbing PE surface. On the basis of

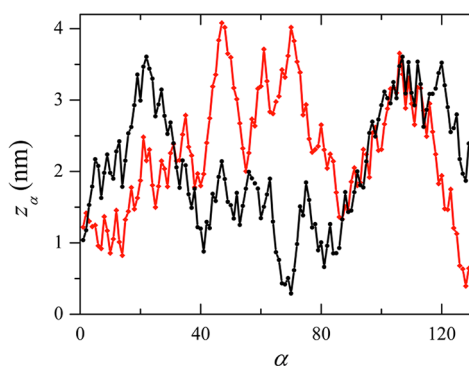


**Figure 5.** Distance between the surface and center of mass of the protein's residues,  $z_{\alpha}$ . The red line corresponds to the first landing ( $t = 1.994$  ns), and the black line corresponds to the third ( $t = 7.529$  ns), respectively.

these distances, we identify the landing sites as the residues (14 and 126–129) in the first landing and (67–71, 81) in the third landing. (For clarity of presentation in the Figure, we do not present the results for the second landing.) The landing sites are composed of residues of different hydrophobicity, for example, hydrophilic Arg14, 128 and hydrophobic Gly126, Cys127, and Leu129 (first landing); hydrophilic Arg68 and hydrophobic Gly67, 71 (third landing). The hydrophobicity of the residues, as described by the hydrophobicity scale,<sup>23,24</sup> does not provide a sufficiently clear quantitative analysis of hydration

to interpret the orientation effects on the adsorption of lysozyme. Instead, in Figure 6, we show the interaction energy

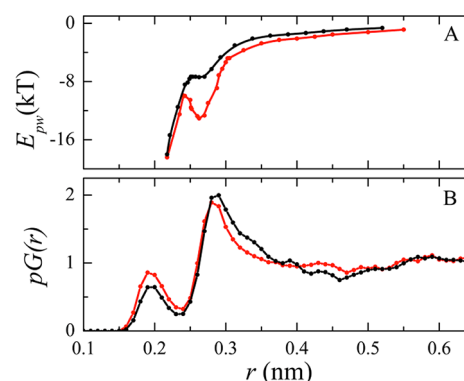


**Figure 6.** (A) Bulk interaction energy between the water and the residues involved in the first (14 and 126–129, in red) and third (67–71, 81, in black) landing, respectively. (B) Proximal radial distribution function,  $pG(r)$ , corresponding to the same two landing sites.

( $E_{pw}$ ) between the residues in the adsorbing sites and the water, along with the corresponding proximal radial distribution function  $pG(r)$ .<sup>13,20–22</sup> These quantities were calculated for the fully solvated protein. Figure 6A shows that the residues involved in the first landing are more attracted to the water than those involved in the third landing. On the proximal radial distribution plot, the small peak at 0.2 nm represents the hydrogen bond between the oxygen atoms of water molecules and hydrogen atoms belonging to the protein, whereas the large peak at  $\sim 0.3$  indicates water molecules acting as hydrogen bond donors. The comparison between the first and third landing sites in Figure 6B shows a larger density of water as hydrogen bonding acceptors at  $r \approx 0.2$  nm. These results suggest that both protein–water and protein–surface interactions play a competitive role affecting the adsorption dynamics.

A visualization of this argument is presented in Figure 7 that shows the change in the protein–surface interactions,  $E_{ps}$ , during the first landing.  $E_{ps}$  shows that the protein feels a relatively strong attraction ( $\sim -45$  kJ/mol) to the surface. However,  $E_{ps}$  undergoes a sudden jump as the protein starts to diffuse away from the PE substrate. The largest change in  $E_{ps}$ , which occurs at  $t \approx 2$  ns, is of 37 kJ/mol and is almost instantaneous

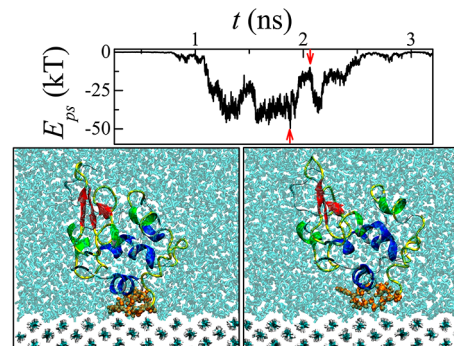


**Figure 7.** Top panel shows the protein–surface interaction energy,  $E_{ps}$ , as a function of time. The two red arrows indicate the times of relevant events during this unsuccessful adsorption attempt, 1.994 and 2.058 ns. The two bottom panels show snapshots of the system at the indicated times. The residues characterized as the landing site (14 and 126–129) are shown in orange.

as it spans a lapse smaller than 0.1 ns. Inspection of the two snapshots (Figure 7) shows that the water molecules reoccupy the space between the protein and the PE surface, as the lysozyme is repelled away from the PE surface. These results indicate that protein adsorption is the result of competitive processes, including the hydration of the protein, the hydration of the substrate PE surface, the protein–surface interactions, and the water–water interactions.

A further understanding of the competition between protein–surface interactions and hydration can be achieved by comparing the magnitudes of the interaction energy of each of the processes. Because of the large amount of water molecules and protein structural flexibility in the aqueous environment, the total interaction energy of the system and the number of water molecules within the first hydration shell undergo large fluctuations and the estimation of the energetic contributions including water molecules is difficult. Therefore, we consider the change in hydration energy of the surface and the change in hydration energy of the residues that get closer to the surface when the protein bounces and compare them to the bare protein–surface interactions. It is observed that there is an increase of 22 water molecules within the first hydration shell surrounding the residues 14 and 126–129, which are the closest to the surface for the first landing attempt. We estimate the change of protein hydration energy based on the hydration numbers at the two relevant time frames (1.994 and 2.058 ns) by using simulations of lysozyme in bulk solution, that is, without the presence of the surface. The change in the protein hydration energy is about  $-74$  kT. The change of PE surface hydration is about  $-28$  kT, which is estimated from the simulations of PE in contact with water without the presence of the protein. The change in the protein surface interactions,  $\Delta E_{\text{ps}}$ , is  $\sim 37$  kT. The protein and surface hydration energy and the protein–surface interactions have comparable magnitudes. It is clear that the hydration of both the protein and the surface play an important role in protein adsorption and affect the protein's orientation-dependent adsorption behavior; therefore, whereas it is hard to estimate its exact magnitude, it should not be ignored.

It is important to emphasize that to obtain the driving force for successful or unsuccessful surface approaches the proper quantity to calculate would be the potential of mean force, namely, the free energy profile as the protein approaches the surface. There are different methodologies to perform such simulations.<sup>25</sup> However, for proteins of the size of interest here, this is a phenomenal task for atomistic simulations, and it is not clear that such calculation would provide the insights obtained from the dynamical simulations. In particular, the role and time scale for dehydration would be very hard to capture in a simulation with a bias toward the minimal (local) free energy state.

## CONCLUSIONS

We have studied lysozyme adsorption on PE surfaces in an aqueous environment using a series of full atomistic MD simulations, starting with different initial orientations. Our previous work<sup>13</sup> showed that the adsorption consists of three stages: diffusion, water depletion, and prolonged structural deformation. In this work, we show the lysozyme's orientation-dependent adsorption behavior, including the initial diffusion and water depletion and also highlight the effects of protein and substrate surface's hydration on protein adsorption.

Lysozyme is most likely to be adsorbed after a side-on landing, for which the protein–PE attractions are very strong. Our results suggest that the protein–surface interaction is not the only governing factor for the adsorption process. Water depletion, as a necessary stage of protein adsorption on hydrophobic surfaces, affects the adsorption kinetics and the asymmetric orientation distribution of the adsorbed lysozyme molecule on the substrate surface. Adsorption with tilted landing is observed to be more rapid than side-on landing because there are fewer water molecules that need to be depleted from the region between the protein and the surface. The energy barrier for the adsorption mainly arises from protein hydration in the first hydration shell as well as from substrate surface hydration. The protein cannot be adsorbed even though the substrate surface exhibits attraction, whenever the protein–surface interaction energy is not large enough to overcome the barrier of breaking the hydration shells. The height of the barrier is strongly orientation-dependent due to the combined effect of hydration and bare protein–surface angular-dependent attraction.

The adsorption process is governed by the competition between protein–surface interactions, protein hydration, substrate surface hydration, and the water–water interactions. The understanding of the adsorption process on the fully atomistic scale is very important for the development of the coarse-grained model, theoretical work, and the experimental antifouling surface design. In particular the role that the hydration interactions play has to be included in simplified models because they are an essential factor determining the type and amount of adsorbed proteins.

## AUTHOR INFORMATION

### Corresponding Author

\*E-mail: igalsz@northwestern.edu.

### Notes

The authors declare no competing financial interest.

## ACKNOWLEDGMENTS

This work was financially supported by NIH grant R01 EB005772. M.A.C. acknowledges support from NSF grant CHE-0957653. This research was partially supported through the computational resources and staff contributions provided by the Quest high performance computing facility at Northwestern University, which is jointly supported by the Office of the Provost, the Office for Research, and Northwestern University Information Technology.

## REFERENCES

- (1) Messersmith, P. B. *Science* **2008**, *319*, 1767–1768.
- (2) Lasseter, T. L.; Clare, B. H.; Abbott, N. L.; Hamers, R. J. *J. Am. Chem. Soc.* **2004**, *126*, 10220–10221.
- (3) Basset, C.; Harder, C.; Vidaud, C.; Dejumat, C. *Biomacromolecules* **2010**, *11*, 806–814.
- (4) Wei, T.; Kaewtathip, S.; Shing, K. J. *Phys. Chem. C* **2009**, *113*, 2053–2062.
- (5) Kim, D. T.; Blanch, H. W.; Radke, C. J. *Langmuir* **2002**, *18*, 5841–5850.
- (6) Su, T. J.; Green, R. J.; Wang, Y.; Murphy, E. F.; Lu, J. R.; Ivkov, R.; Satija, S. K. *Langmuir* **2000**, *16*, 4999–5007.
- (7) Sousa, S. R.; Moradas-Ferreira, P.; Saramago, B.; Melo, L. V.; Barbosa, M. A. *Langmuir* **2004**, *20*, 9745–9754.
- (8) Shaw, D. E.; Maragakis, P.; Lindorff-Larsen, K.; Piana, S.; Dror, R. O.; Eastwood, M. P.; Bank, J. A.; Jumper, J. M.; Salmon, J. K.; Shan, Y. B.; Wriggers, W. *Science* **2010**, *330*, 341–346.

- (9) Zheng, J.; Li, L. Y.; Chen, S. F.; Jiang, S. Y. *Langmuir* **2004**, *20*, 8931–8938.
- (10) Raffaini, G.; Ganazzoli, F. *Langmuir* **2004**, *20*, 3371–3378.
- (11) Wei, T.; Mu, S. J.; Nakano, A.; Shing, K. *Comput. Phys. Commun.* **2009**, *180*, 669–674.
- (12) Sun, Y.; Welsh, W. J.; Latour, R. A. *Langmuir* **2005**, *21*, 5616–5626.
- (13) Wei, T.; Carignano, M. A.; Szleifer, I. *Langmuir* **2011**, *27*, 12074–12081.
- (14) Kubiak-Ossowska, K.; Mulheran, P. A. *Langmuir* **2010**, *26*, 7690–7694.
- (15) Kubiak, K.; Mulheran, P. A. *J. Phys. Chem. B* **2009**, *113*, 12189–12200.
- (16) Hess, B.; Kutzner, C.; van der Spoel, D.; Lindahl, E. *J. Chem. Theory Comput.* **2008**, *4*, 435–447.
- (17) Jorgensen, W. L.; Maxwell, D. S.; TiradoRives, J. *J. Am. Chem. Soc.* **1996**, *118*, 11225–11236.
- (18) Jorgensen, W. L.; Chandrasekhar, J.; Madura, J. D.; Impey, R. W.; Klein, M. L. *J. Chem. Phys.* **1983**, *79*, 926–935.
- (19) Ceresoli, D.; Righi, M. C.; Tosatti, E.; Scandolo, S.; Santoro, G.; Serra, S. *J. Phys.: Condens. Matter* **2005**, *17*, 4621–4627.
- (20) Merzel, F.; Smith, J. C. *Proc. Natl. Acad. Sci. U.S.A.* **2002**, *99*, 5378–5383.
- (21) Lounnas, V.; Pettitt, B. M.; Phillips, G. N. *Biophys. J.* **1994**, *66*, 601–614.
- (22) Makarov, V.; Pettitt, B. M.; Feig, M. *Acc. Chem. Res.* **2002**, *35*, 376–384.
- (23) Kyte, J.; Doolittle, R. F. *J. Mol. Biol.* **1982**, *157*, 105–132.
- (24) Rose, G. D.; Wolfenden, R. *Annu. Rev. Biophys. Biomol. Struct.* **1993**, *22*, 381–415.
- (25) Trzesniak, D.; Kunz, A. E.; van Gunsteren, W. F. *Chem. Phys. Chem.* **2007**, *8*, 162.